

# Nanoporous Polyimides Derived from Highly Fluorinated Polyimide/Poly(propylene Oxide) Copolymers

Kenneth R. Carter,\* Richard A. DiPietro, Martha I. Sanchez, and Sally A. Swanson

IBM Research Division, Almaden Research Center, 650 Harry Road,  
San Jose, California 95120-6099

Received November 8, 1999. Revised Manuscript Received October 31, 2000

Porous, low dielectric constant polyimide films have been made by a “nanof foam” approach. The pore sizes generated in the polymer films are in the tens of nanometers range, hence the term “nanof oams”. The nanoporous foams are generated by preparing triblock copolymers with the majority phase comprising polyimide and the minor phase consisting of a thermally labile block. Films of the copolymers are cast and then heated to effect solvent removal and annealing, resulting in microphase separation of the two dissimilar blocks. The labile blocks are selectively removed via thermal treatments, leaving pores the size and shape of the original copolymer morphology. The polyimide derived from 2,2-bis(4-aminophenyl)hexafluoropropane (6FDA) and 9,9-bis(trifluoromethyl)xanthenetetracarboxylic dianhydride (6FXDA) was used as the matrix material for the generation of nanof oams, and specially functionalized poly(propylene oxide) oligomers were used as the thermally labile constituent. The synthesis and characterization of the copolymers were performed and the process for obtaining nanof oams was optimized. The foams were characterized by a variety of techniques including thermal gravimetric analysis (TGA), transmission electron microscopy (TEM), dynamic mechanical thermal analysis (DMTA), density, small-angle X-ray scattering (SAXS), refractive index, and dielectric constant measurements. Thin-film, high-modulus nanoporous films with good mechanical properties and dielectric constants  $\sim 2.3$  have been synthesized by the copolymer/nanof oam approach.

## Introduction

In recent years there has been an explosion in the amount of research in the areas of nanotechnology and nanostructured materials, with the ultimate aim being the ability to control the construction of novel molecular devices possessing extraordinary properties. This nanoscopic fashioning and design of materials for specific applications is being done by this relatively new “bottoms-up” approach of building useful materials by the controlled manipulation of individual atoms or molecules.<sup>1</sup> With that in mind, we set about investigating ways of using nanostructured materials to develop new materials for microelectronic device manufacture.

There currently exists a need for new intermetal dielectric layers (IMD) with lower dielectric constants in order to reduce the signal delays, drive voltages, and power consumption of today’s high-powered integrated circuits (ICs). To this end, we are actively in search of low dielectric constant materials that can be incorporated into integrated circuit production.

The most commonly used IMD material today is silicon dioxide (SiO<sub>2</sub>), which has a dielectric constant ( $\epsilon$ ) of  $\sim 4.0$ . Current specifications for new insulating films call for materials with dielectric constants between 3 and 3.3, and within the next decade, devices may require materials with dielectric constants approaching

2.0 or below. While there are a number of possible candidate materials for current uses, the list of viable materials with dielectric constants  $< 3.0$  is more limited. The greatest limitations in materials qualification are the stringent IC processing conditions (thermal stability, resistance to chemical/mechanical treatments, mechanical stability, ease of use, etc.).<sup>2,3</sup>

High-performance polymers, such as polyimides, polyesters, and aramids, have found a number of uses in a variety of electronic devices and components.<sup>4</sup> The use of polyimides, in particular, can be attributed to their many favorable properties such as high thermal stability, ease of processing, low stress/coefficient of thermal expansion (CTE), and very good electrical properties (lower dielectric constant, high resistivity and high breakdown voltage).

One of the most commonly employed polyimides, Kapton pyromellitic dianhydride/oxydianiline (PMDA/ODA), has a dielectric constant of 3.2 (measured at 1 MHz). A variety of approaches have been studied to synthesize polyimides with lower dielectric constants. The most common approach has been to develop materials high in organofluorine content, often by the

(1) Ball, P. *Made to Measure: New Materials for the 21<sup>st</sup> Century*; Princeton University Press: Princeton, NJ, 1998.

(2) Monnig, K. A. In *Proceedings of SEMATECH—Low Dielectric Constant Materials and Interconnects Workshop*; San Diego, CA, 1996; SEMATECH: Austin, TX.

(3) Murarka, S. P. *Solid State Technol.* **1996**, 3, 83.

(4) *Polymers for Electronic Applications*; Lai, J. H., Ed.; CRC Press: Boca Raton, FL, 1989.

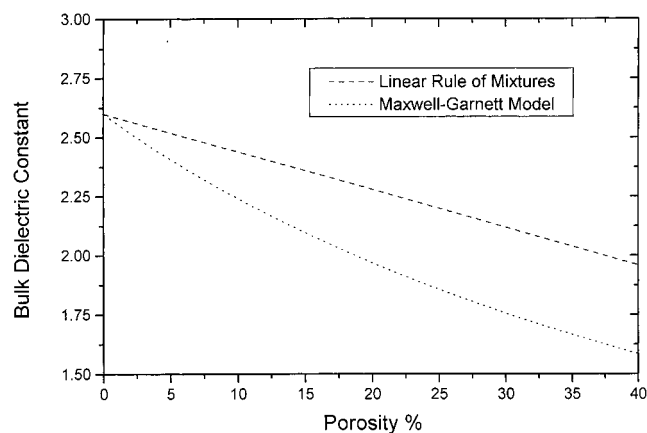


**Figure 1.** Calculated effect of porosity on bulk dielectric constant.

incorporation of pendant perfluoroalkyl groups. For example, researchers at Hoechst<sup>5</sup> developed "Sixef" polyimide, which contains hexafluoroisopropylidene linkages and has a dielectric constant of 2.6. Auman and Trofimenko<sup>6,7</sup> have reported the synthesis of a number of polyimides based upon the fluorinated rigid cyclic dianhydrides 9,9-bis(trifluoromethyl)xanthenetetracarboxylic dianhydride (6FXDA) and 3FXDA, with dielectric constants as low as 2.5. The methodology for developing new, highly fluorinated polyimides can be limited, to a certain extent, by synthetic difficulties associated with the incorporation of greater amounts of pendant perfluoroalkyl groups.

An alternative approach toward lowering a polymer's bulk dielectric constant is to introduce nanoscopic porosity into the polymer film. The effect of porosity on the dielectric constant of a material can be quite dramatic, with observed lowering of dielectric constant greater than predicted by a linear rule-of-mixtures model. Indeed, the Maxwell-Garnett approximation<sup>8</sup> is one of the most widely used methods for calculating the bulk dielectric properties of inhomogeneous materials.<sup>9,10</sup> Figure 1 depicts the predicted bulk dielectric constant of a material as a function of porosity.

In porous polymers designed for use in microelectronics devices, the pore sizes must be much smaller than the film thickness or any microelectronic features, i.e.,  $\ll 100$  nm. Additionally, the porous polymer should possess as many of the favorable properties of the parent material as possible (i.e., stability under conditions of fabrication and use). While there are a variety of approaches reported for the foaming of polyimides, such as the use of foaming agents,<sup>11-13</sup> partial degradation generating a foaming agent,<sup>14,15</sup> the inclusion of hollow

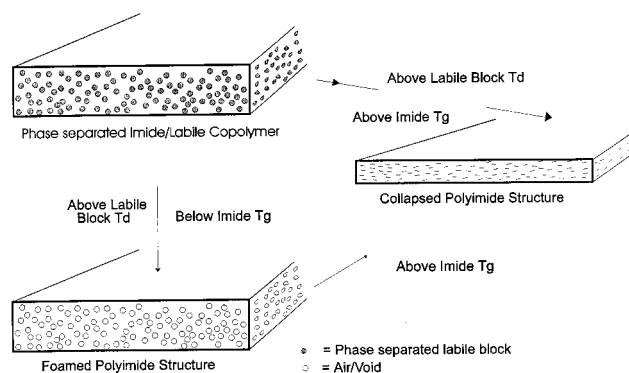


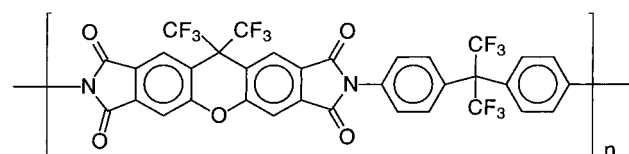
**Figure 2.** Preparation of polyimide nanofoams by the phase-separated block copolymer route.

microspheres,<sup>16</sup> and microwave processing,<sup>17</sup> most of these methods leave materials with large void sizes and open pore structures, making them poor candidates for use in microelectronic devices.

Previous reports have outlined the synthesis of porous structures of high-temperature thermoplastic materials by utilizing a block copolymer approach.<sup>18,19</sup> In these systems the pore sizes are in the nanometer range, hence the term "nanofoam". The nanoporous materials are prepared from block copolymers consisting of thermally stable and thermally labile blocks, the latter being the dispersed phase. Pore formation is effected by thermolysis of the thermally labile block, leaving pores of size and shape corresponding to that of the initial copolymer morphology (Figure 2). The ultimate dielectric constant achievable is limited primarily by two factors, the intrinsic dielectric constant of the polyimide matrix and the morphology and stability of the porous structure (usually a  $\sim 25$ – $30\%$  porosity maximum).

We now report the exploration of nanofoams using 6FXDA/6FDAm polyimide (dielectric constant  $\sim 2.6$ ) as the matrix material (Chart 1). We believe that the intro-

**Chart 1**



**6FXDA/6FDAm Polyimide (1)**

duction of porosity into this polymer with an intrinsic dielectric constant of 2.6 will give us access to usable thin films with dielectric constants approaching 2.0.

### Experimental Section

**Materials.** All materials were commercially available unless otherwise noted. 2,2-Bis(4-aminophenyl)hexafluoropro-

(5) Haider, M.; Chenevey, E.; Vora, R. H.; Cooper, W.; Glick, M.; Jaffe, M. *Mater. Res. Soc. Symp. Proc.* **1991**, 227, 379.

(6) Auman, B. C.; Trofimenko, S. *Polym. Prepr. (Am. Chem. Soc., Div. Polym. Chem.)* **1992**, 34 (2), 244.

(7) Auman, B. C. In *Advances in Polyimide Science and Technology*; Proceedings of the 4th International Conference on Polyimides, 1991; Feger, C., Khojasteh, M. M., Htoo, M. S., Eds.; Technomic: Lancaster, PA, 1993; pp 15–32.

(8) Garnett, J. C. M. *Philos. Trans. R. Soc. London, Ser. B* **1904**, 203, 385.

(9) Bergman, D. J.; Stroud, D. *J. Phys., Solid State Phys.* **1992**, 46, 147.

(10) Cha, H. J.; Hedrick, J. L.; DiPietro, R. A.; Blume, T.; Beyers, R.; Yoon, D. Y. *Appl. Phys. Lett.* **1996**, 68, 1930.

(11) Smearing, R. W.; Floryan, D. C. U.S. Patent 4,535,365 to General Electric, 1985.

(12) Krutchén, C. M.; Wu, P. U.S. Patent 4,535,100 to Mobil Oil, 1985.

(13) Hoki, T.; Matsuki, Y. European Patent 186308 to Asahi Chemical Co., 1986.

(14) Meyers, R. A. *J. Polym. Sci., Part A-1* **1969**, 7, 2757.

(15) Carleton, P. S.; Farrissey, W. J.; Rose, J. S. *J. Appl. Polym. Sci.* **1972**, 16, 2983.

(16) Narkis, M.; Paterman, M.; Boneh, H.; Kenig, S. *Polym. Eng. Sci.* **1982**, 22, 417.

(17) Gagliani, J.; Supkis, D. E. *Adv. Astronaut. Sci.* **1979**, 38, 193.

(18) Carter, K. R.; DiPietro, R. A.; Sanchez, M. I.; Russell, T. P.; Lakshmanan, P.; McGrath, J. E. *Chem. Mater.* **1997**, 9, 105.

(19) Hedrick, J. L.; Carter, K. R.; Richter, R.; Miller, R. D.; Russell, T. P.; Flores, V.; Meccerreyes, D.; Dubois, P.; Jérôme, R. *Chem Mater.* **1998**, 10 (1), 39.

pane (6FDAm) (Chriskev Co.) was sublimed  $2\times$  prior to use. The rigid dianhydride monomer 9,9-bis(trifluoromethyl)xanthetetracarboxylic dianhydride (6FXDA)<sup>7</sup> was purchased from DuPont Chemical Co., and sublimed prior to use. Hydroxy-terminated poly(propylene oxide) of nominal molecular weights 5000 and 10 000 g/mol were kindly supplied by the Dow Chemical Co. *N*-Methyl-2-pyrrolidinone (NMP) was distilled under vacuum from P<sub>2</sub>O<sub>5</sub>.

**Characterization.** NMR spectra (in DMSO-*d*<sub>6</sub> or CDCl<sub>3</sub>) were recorded on an IBM WP 250 spectrometer operating at 250.1 MHz (<sup>1</sup>H) and 62.9 MHz (<sup>13</sup>C) with chemical shifts reported in parts per million (ppm) downfield from tetramethylsilane.

Polymer films for mechanical and thermal analysis were cast from NMP and heated to remove solvent and anneal the polymer. Glass transition temperatures, taken as the midpoint of the change in slope of the baseline, were measured on a DuPont DSC 1090 instrument at a heating rate of 10 °C/min (N<sub>2</sub>). Thermal gravimetric analyses (TGA) (N<sub>2</sub> and air) of the polymer films were conducted on a Perkin-Elmer model TGA-7 at a heating rate of 10 °C/min, or isothermal weight loss was measured at different temperatures over a 4–10 h period. Dynamic mechanical measurements were made with a Polymer Laboratories dynamic mechanical thermal analyzer (DMTA) in the tension mode with a heating rate of 10 °C/min (10 Hz). Density measurements were obtained with a density gradient column composed of water and calcium nitrate. The column was calibrated against a set of beads of known densities (Scientific Glass & Instruments, Inc.) and maintained at 25 °C ( $d = 1.05\text{--}1.45$ ). At least two specimens were used for each density measurement.

Small-angle X-ray scattering studies (SAXS) were performed on beamline I-4 at the Stanford Synchrotron Radiation Laboratory. Details of the beamline optics are described elsewhere.<sup>20</sup> Samples were prepared by placing stacks of thin films in a sample cell with Kapton windows. Standard procedures were used to correct the scattering profiles for parasitic scattering, electronic noise, and sample absorption. Scattering profiles will be presented as a function of the scattering vector,  $q$ , which is given by  $(4\pi/\lambda) \sin \theta$ , where  $\lambda$  is the wavelength and  $2\theta$  is the scattering angle.

Transmission electron microscopy (TEM) was performed on a Philips 420T scanning transmission electron microscope operating at 100 kV. The polymer samples were embedded in an epoxy resin and microtomed in cross section. The resulting sections were between 500 and 1000 Å thick.

Refractive index values were obtained on 2–3 μm thick samples spin coated onto quartz or gold-coated quartz wafers, which were then cured and foamed. Measurements were made on a Metricon Prism Coupler (PC-2000), which is an optical waveguide technique providing both in-plane and out-of-plane refractive indices.

**4-Aminophenyl Carbonate-Terminated Poly(propylene Oxide).** The 4-aminophenyl carbonate-terminated poly(propylene oxide) oligomers were prepared by reacting a 5-fold excess of nitrophenyl chloroformate with hydroxy-terminated propylene oxide oligomer (5000 or 10 000 g/mol nominal molecular weight) in THF with pyridine as an acid acceptor. After several hours, the insoluble amine hydrochloride salt was removed by filtration and the 4-nitrophenyl chloroformate complex was reduced by hydrogenation over Pearlman's catalyst. After the reduction, the oligomer was washed with water. This procedure yielded oligomer of 3400 or 13 200 g/mol as determined by <sup>1</sup>H NMR and potentiometric titration with perchloric acid.

**6FXDA/6FDAm Polyimide (1).** A 25 mL three-neck flask fitted with an overhead stirrer and charged with 1.191 g (3.56 mmol) of 6FDAm and 10 mL of cyclohexanone was heated with stirring under an argon blanket to dissolve the diamine. After a homogeneous solution was obtained, the flask was cooled to

5 °C and 1.633 g (3.56 mmol) of 6FXDA was added and washed into the flask with 5 mL of cyclohexanone. The solution was allowed to warm to room temperature and stirred for 24 h. Chemical imidization was accomplished by adding 0.97 g (12 mmol) of pyridine and 1.24 g (12 mmol) of acetic anhydride to the viscous poly(amic acid) solution and heating to 50 °C for 8 h. The resulting viscous polymer solution was cooled to room temperature and precipitated into 800 mL of hexane, washed  $2\times$  in water/methanol, filtered, and vacuum-dried (50 °C at 26 Torr) to constant weight to yield 2.7 g of polymer.

**6FXDA/6FDAm-co-Poly(propylene Oxide) Triblock Copolymers (2c–8c).** A number of triblock copolymers with variations in poly(propylene oxide) content and hence relative block lengths were synthesized. A representative example for the synthesis of 6FXDA/6FDAm-co-poly(propylene oxide) triblock copolymer is given.

The triblock copolymers were prepared in a one-pot/two-stage process in which the polyamic acid precursor is formed and chemically imidized, yielding the appropriate imide/propylene oxide copolymers. A representative example follows: A 50 mL three-neck flask fitted with an overhead stirrer was charged with 2.367 g (5.16 mmol) of 6FXDA, 1.679 g (5.023 mmol) of 6FDAm, 0.96 g (0.28 mmol) of a 3.4K MW aminophenyl carbonate-terminated poly(propylene oxide) oligomer, and 35 mL of cyclohexanone. The contents of the flask were allowed to stir for 24 h under argon, and the mixture became a clear, yellow homogeneous solution. At this point, 1.11 g (14 mmol) of pyridine and 1.46 g (14 mmol) of acetic anhydride were added and the mixture was heated to 80 °C for 12 h to effect chemical imidization. The resulting viscous polymer solution was cooled to room temperature and precipitated into 800 mL of hexane, washed  $2\times$  in water/methanol, filtered, and vacuum-dried (50 °C at 26 Torr) to constant weight to yield 4.8 g of polymer.

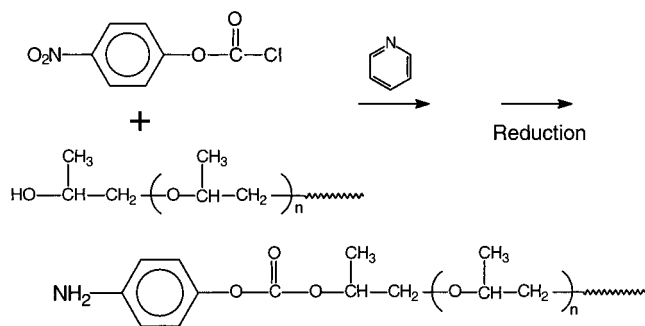
**Pore Formation.** Pore formation is achieved in a two-step process. First, the 6FXDA/6FDAm-co-poly(propylene oxide) triblock copolymers (**2c–8c**) were dissolved in cyclohexanone at concentrations of 10–20% solids. Thin films could be formed by spinning (1–10 μm) or doctor blading (10–40 μm) onto an appropriate substrate. The films were then heated incrementally to 310 °C in an inert atmosphere (argon) or under high vacuum to effect solvent removal and densification of the copolymer. The second step involves the thermolysis and removal of the labile block, poly(propylene oxide), by heating the copolymer in the presence of oxygen at 250 °C for 10–12 h, yielding the porous polyimides **2f–8f**.

## Results and Discussion

The block copolymer approach used to generate polyimide nanofoams requires well-defined block segments, which include both the thermally stable matrix block (imide) and the thermally labile block [poly(propylene oxide)]. A critical requirement of the labile block segments is that they must undergo a controllable and quantitative degradation into low molecular weight products, which must, in turn, diffuse easily through the polyimide matrix. Because the decomposition of the poly(propylene oxide) blocks is thermally initiated, it is equally important that the poly(propylene oxide) decomposition temperature,  $T_{dec}$ , be below the softening temperature,  $T_{soft}$ , of the 6FXDA/6FDAm matrix in order to prevent collapse of the developing structure. The labile block must also possess sufficient thermal stability to allow film annealing and solvent removal. The temperature  $T_{soft}$  is related to the  $T_g$  of the matrix and takes into account softening due to plasticization caused by dissolved poly(propylene oxide) decomposition byproducts. Lowering of the matrix  $T_g$  due to plasticization has been observed to be small, on the order of 5–10 °C. The temperature difference between poly(propylene

(20) Russell, T. P. in *Handbook of Synchrotron Radiation*; Brown, G. S., Moncton, D. E., Eds.; North-Holland: Amsterdam, 1991; Vol. 3.

### Scheme 1. Functionalization of Poly(propylene oxide)



oxide) degradation,  $T_{\text{dec}}$ , and matrix polyimide softening,  $T_{\text{soft}}$ , is referred to as the "processing window". Poly(propylene oxide) possesses sufficient thermal stability at 310 °C, under an inert atmosphere, to permit film preparation and annealing. The fact that poly(propylene oxide) has effectively two  $T_{\text{dec}}$ , one under oxidative conditions and another under inert conditions, makes it especially well suited as a labile block in this process. After copolymer film formation at 310 °C, the poly(propylene oxide) can be thermally degraded at temperatures lower than 310 °C, preferably at ~250 °C, in the presence of atmospheric oxygen.

Though 6FXDA/6FDAm polyimide has a reported  $T_g$  of 422 °C,<sup>7</sup> the  $T_g$  is cure-dependent, with observed  $T_g$  tracking its curing history. For example, if a sample film is prepared and heated to 350 °C, that sample will have an observed  $T_g$  of 350 °C. If that same sample is subsequently heated to 375 °C, the film's  $T_g$  will rise to that temperature. Therefore, to obtain a high  $T_g$  with this material, it is necessary to cure the sample at the highest temperature possible. This memory effect has several ramifications for the curing of 6FXDA/6FDAm-co-poly(propylene oxide) triblock copolymers. Curing temperature for poly(propylene oxide)-containing copolymers is limited to  $T_{\text{dec}}$  or 310 °C, meaning that the  $T_g$  of the matrix at that point is also 310 °C. Therefore, for this system, the pore formation processing window is between 250 ( $T_{\text{dec}}$ ) and 305 °C ( $T_{\text{soft}}$ ).

The successful use of poly(propylene oxide) to make triblock copolymers required the synthesis of suitable amine-terminated poly(propylene oxide) oligomers. The availability of hydroxy-terminated poly(propylene oxide) allowed us to explore methods of functionalizing end groups to give the desired amine-terminated oligomers (Scheme 1). The aromatic amine-terminated poly(propylene oxide) derivatives prepared for this study contained an aminophenyl carbonate end group. These oligomers were synthesized by reacting hydroxy-terminated poly(propylene oxide) with 4-nitrophenyl chloroformate in THF in the presence of pyridine. This reaction mixture was filtered to remove the pyridine hydrochloride salts and then reduced with Pearlman's catalyst under  $\text{H}_2$ , yielding 4-aminophenyl carbonate-terminated poly(propylene oxide) oligomers. The completion of oligomer functionalization and isolated molecular weight were determined by both  $^1\text{H}$  NMR and potentiometric titration of amine end groups with perchloric acid. Though the hydroxy-terminated poly(propylene oxide) starting material was either 5000 or 10 000 g/mol, the  $\langle M_n \rangle$  of the functionalized poly(propylene oxide) was

found to vary from 3400 to 13 200 g/mol due to either incomplete functionalization or fractionation of the poly(propylene oxide) upon isolation.

Most polyimides can be prepared via a number of different methods.<sup>21,22</sup> The most common technique is the two-step synthesis in which poly(amic acid) formation is followed by cyclodehydration to the corresponding polyimide. This imidization can be effected by either thermal or chemical means. The polyimide matrix chosen for this study, 6FXDA/6FDAm polyimide, is a rigid/flexible polyimide that is soluble in a variety of polar organic solvents in its fully imidized form. Due to the poor mechanical properties of polymer films derived directly from the curing of polyamic acid solutions of 6FXDA/6FDAm,<sup>7</sup> we chose to study fully imidized A-B-A triblock copolymers composed of 6FXDA/6FDAm (B block) and poly(propylene oxide) (A block).

As shown in Scheme 2, if an aromatic amine-terminated poly(propylene oxide) block is reacted at the proper stoichiometry with 6FXDA and 6FDAm an A-B-A type copolymer is obtained, with poly(propylene oxide) comprising the A blocks. The molecular weight of the poly(propylene oxide) oligomer remains unchanged during the formation of the copolymers. The precisely controlled stoichiometric imbalance, calculated from the Carothers equation, of these condensation reactions provides for control of the length of the polyimide segment and incorporation of poly(propylene oxide) (usually given as weight percent) in these block copolymers. Since monofunctional poly(propylene oxide) oligomer acts as a polyimide chain terminator, we focused our attention on poly(propylene oxide) of molecular weights of 3400–13 200 g/mol. The use of these oligomers with sufficiently high molecular weights provided for the incorporation of a large amount of poly(propylene oxide) into the copolymers while preserving a longer polyimide B segment.

A number of 6FXDA/6FDAm-co-poly(propylene oxide) triblock copolymers were synthesized with variations in the total labile block percentage and block length. The A-B-A polyimide block copolymers could be isolated, stored, characterized (by NMR, DSC, TGA, and GPC), and subsequently redissolved and processed into thin films. Table 1 summarizes the polymers prepared. It was desirable to study copolymers containing 15–30% poly(propylene oxide), which theory would predict would most likely yield isolated microphase-separated domains of poly(propylene oxide) in the polyimide matrix.<sup>23</sup> Though we were able to incorporate lower amounts of poly(propylene oxide) (1–15%), we were more interested in higher levels of labile block incorporation to achieve the best balance between morphology and dielectric and mechanical properties.

Since the triblock copolymers were soluble in suitable solvents,  $^1\text{H}$  NMR was used to determine the amount of poly(propylene oxide) incorporated into each copolymer (see Figure 3). A comparison of the area under the resonances due to the aromatic protons (8.1–7.0 ppm) to the area of the methyl resonance of the poly(propylene oxide) segment (1.0 ppm) allowed the compositions of

(21) Volksen, W. *Adv. Polym. Sci.* **1994**, *117*, 111.

(22) Mittal, K., Ed. *Polyimides: Synthesis, Characterization and Application*; Plenum Press: New York, 1984; Vols. 1 and 2.

(23) Meier, D. J. *J. Polym. Sci., Part C* **1969**, *26*, 81.



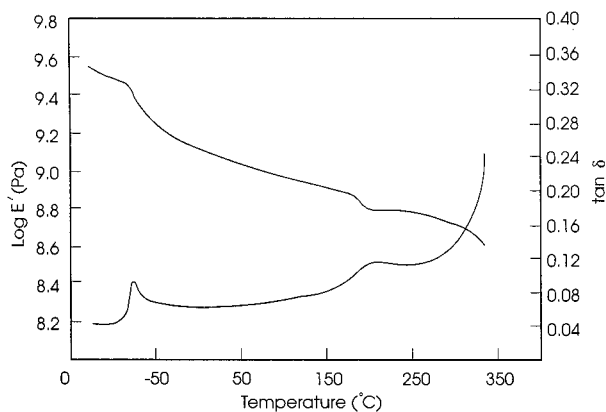


**Figure 4.** DMTA spectrum of a 6FXDA/6FDAm-co-poly(propylene oxide) copolymer.

type of gross phase separation, even at levels lower than 1%. The homopolymer contamination can be the result of unreacted macromonomer or contamination or impurity of any of the monomers. In most cases, small amounts of homopolymer or oligomer can be removed by selective washing of the copolymer after precipitation. Usually this results in a certain amount of fractionation of the triblock polymers, with lower molecular weight fractions being lost during this purification process. In the case of the 13 200 g/mol poly(propylene oxide) block copolymers, there was not sufficient difference between the solubilities of the triblock copolymer and the trace amount of unreacted poly(propylene oxide) oligomer for washings to be effective.

The presence of a phase-separated morphology is supported by DMTA data. The DMTA of a 6FXDA/6FDAm/poly(propylene oxide) copolymer (sample **4c**) is shown in Figure 4. The copolymers all exhibited two transitions, characteristics of a microphase separated morphology. The low-temperature relaxation and slight drop in modulus at  $-60\text{ }^{\circ}\text{C}$  is due to the poly(propylene oxide) phase. The modulus decrease and concurrent increase of  $\tan \delta$  at the  $T_g$  of the polyimide matrix of the phase-separated copolymer is seen at approximately  $310\text{ }^{\circ}\text{C}$ .

The cured copolymers were converted into porous films (**2f–8f**) by heating them to  $250\text{ }^{\circ}\text{C}$  in air for 6–10 h. The poly(propylene oxide) block undergoes oxidative thermolysis, in turn yielding low molecular weight byproducts, which quantitatively diffuse from the film, leaving voids in the polymer matrix. Thermal gravimetric analysis (TGA) was performed to monitor the thermolysis of poly(propylene oxide) from copolymer samples. No detectable residual labile block or poly(propylene oxide) byproducts were observed in the resulting porous polymers, as examined by TGA or infrared spectroscopy (IR). A typical 6FXDA/6FDAm/poly(propylene oxide) copolymer dynamic TGA thermogram is shown in Figure 5. When the copolymer is heated under argon, the thermolysis is monomodal, with complete poly(propylene oxide) removal from the sample occurring by  $450\text{ }^{\circ}\text{C}$ . The polyimide matrix begins to degrade at  $500\text{ }^{\circ}\text{C}$ . When the thermolysis was performed in air, the onset of poly(propylene oxide) degradation was observed at  $220\text{ }^{\circ}\text{C}$  and was bimodal, suggesting two competing thermolysis mechanisms, indicating that there is significant oxidative degradation at this lower temperature followed by thermally induced degradation

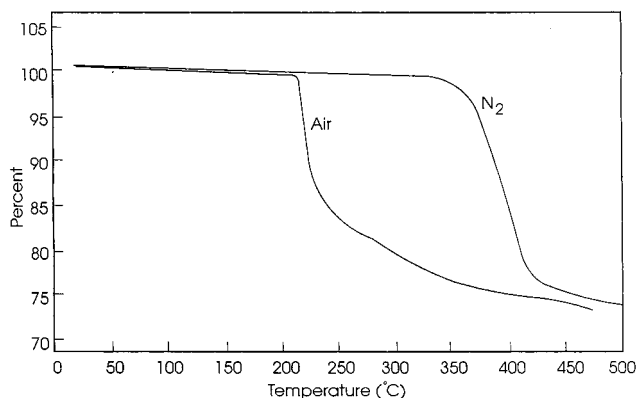


**Figure 5.** TGA of a 6FXDA/6FDAm-co-poly(propylene oxide) copolymer in air and nitrogen.

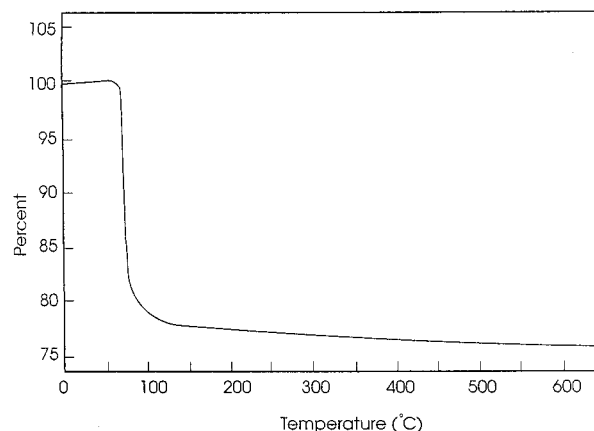


**Figure 6.** Isothermal TGA of a 6FXDA/6FDAm-co-poly(propylene oxide) copolymer heated at  $250\text{ }^{\circ}\text{C}$ .

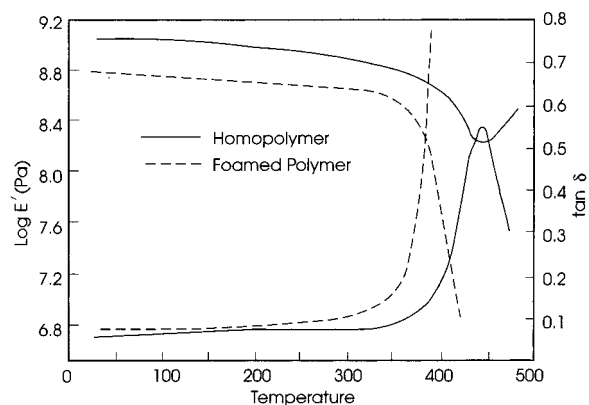


**Figure 7.** DMTA of 6FXDA/6FDAm polyimide and a 6FXDA/6FDAm polyimide nanofoam.

at  $300\text{ }^{\circ}\text{C}$ . Isothermal TGA (Figure 6) was performed to establish the best conditions for complete thermolysis and removal of the poly(propylene oxide) segments. The TGA experiments helped establish that heating the samples at  $250\text{ }^{\circ}\text{C}$  for  $>6\text{ h}$  in air was sufficient for quantitative removal of poly(propylene oxide) from the samples, a temperature far below the softening point of the matrix.

The storage modulus and  $\tan \delta$  of the polymers were determined as a function of temperature by DMTA. The DMTA of 6FXDA/6FDAm polyimide homopolymer and a 6FXDA/6FDAm polyimide nanofoam (**4f**) are shown in Figure 7. In this case, both samples **1** and **4f** had been annealed to  $400\text{ }^{\circ}\text{C}$  prior to examination. The

**Table 2. 6FXDA/6FDAm Polyimide Nanofoam Density Measurements**

	PO block (Mn)	PO volume % <sup>a</sup>	foaming temp, °C	density, g/cm <sup>3</sup>	porosity, %	pore efficiency
<b>1</b>	<i>b</i>	0		1.49		
<b>2f</b>	3400	22	250	1.23	18	80
<b>3f</b>	3400	25	250	1.21	19	78
<b>4f</b>	3400	31	250	1.19	20	66
<b>5f</b>	13 200	16	250	1.31	11	69
<b>6f</b>	13 200	22	250	1.32	10	45
<b>7f</b>	13 200	32	250	1.21	18	56
<b>8f</b>	13 200	35	250	1.13	24	68

<sup>a</sup> Volume % was calculated from weight %, with the relative densities of the two phases taken into account. <sup>b</sup> Homopolymer.

polyimide nanofoams possess a high modulus ( $E = 630$  MPa) and have high  $T_g$  values (375 °C compared to >400 °C for the homopolymer). This modest depression in modulus and  $T_g$  is not surprising since the sample has a level of porosity of greater than 15%.

Porosity and void formation were determined from density, refractive index, and small-angle X-ray scattering measurements. The physical characteristics of the porous 6FXDA/6FDAm polyimides **2f–8f** are shown in Table 2. In most of the samples, the volume fraction of poly(propylene oxide) in the copolymers tracked nicely with the volume fraction of pores observed after pore generation. Conversion of the volume of poly(propylene oxide) in the copolymers into porous regimes (i.e., the pore formation efficiency as measured by volume fraction of labile block) was usually ~80%, with the partial collapse of the pores being attributed to stress-induced collapse caused by plasticization of the stressed polyimide matrix by the labile block degradation products. The 6FXDA/6FDAm polyimide nanofoams that were derived from copolymers with a moderate level of poly(propylene oxide) incorporation show good pore conversion, while the copolymers with higher levels of incorporation showed noticeable low pore conversion efficiency. The noted efficiencies can most likely be attributed to the morphology of the parent copolymers. Copolymers with higher levels of 3400 poly(propylene oxide) blocks or the large, micrometer-sized phase separated domains observed in the 13 200 poly(propylene oxide) blocks copolymers (**5c–8c**) result in large, highly interconnected domains. Upon thermolysis, these highly porous matrixes are more likely to undergo stress-induced collapse, resulting in porosity levels well below what would be predicted on the basis of labile block incorporation.

The presence of pores in the size regime of ~10 nm in samples **2f–4f** has been confirmed by TEM and small-angle X-ray scattering studies. SAXS experiments were performed on the parent 6FXDA/6FDAm-*co*-poly(propylene oxide) triblock copolymers and on the nanoporous samples after thermolysis of the poly(propylene oxide) blocks. A typical scattering profile is shown in Figure 8. Here the scattering of a copolymer (**3c**) containing 22 wt % poly(propylene oxide) is shown as a function of the scattering vector  $q$ , which is given by  $(4\pi/\lambda) \sin \theta$ , where  $\lambda$  is the wavelength and  $2\theta$  is the scattering angle. For all of the copolymers, the SAXS profile shows a monotonic decrease in the scattering as a function of  $q$ . In a disordered, microphase-separated material where there are no long-range correlations in

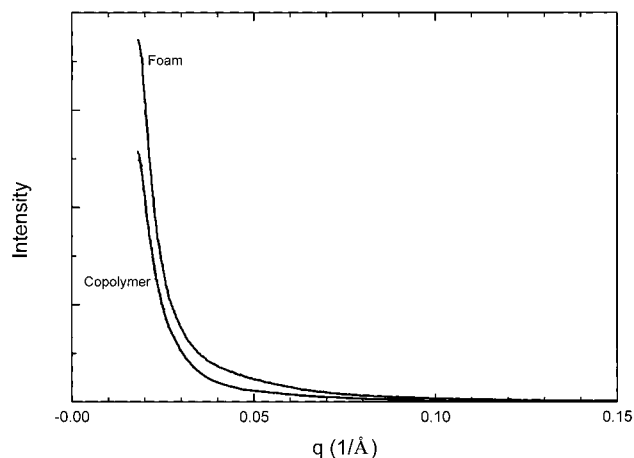


**Figure 8.** Small-angle X-ray scattering (SAXS) results for 6FXDA/6FDAm-*co*-poly(propylene oxide) copolymer and 6FXDA/6FDAm polyimide nanofoam.

the spatial distribution of the poly(propylene oxide) domains, this type of result is expected. This is further evidence that the copolymer has microphase-separated but is trapped in a highly nonequilibrium state. From a Debye–Beuche analysis,<sup>24</sup> a correlation length can be determined that, when the volume fraction of the phases is taken into account, allows for the calculation of average domain size. An average size of the poly(propylene oxide) domains of ~10 nm was obtained for copolymer systems ranging in composition from 17% to 25%. Defining the size of the domains with any greater precision is not reasonable given the assumptions. The important observation is that a nanophase-separated morphology is observed. After degradation of the poly(propylene oxide), a porous structure (**3f**) is generated, evident by the dramatic increase in the scattering. As with the parent copolymers, the scattering from the nanofoams decreases monotonically with  $q$ . It is important to note that the angular dependence of the scattering does not significantly change. This indicates that the size and the spatial distribution of the nanoscopic domains does not change, rather only the contrast between the matrix and the dispersed domains undergoes a dramatic increase. This result clearly shows that the poly(propylene oxide) domains are transformed into air pores of the same size and morphology.

A TEM micrograph of a nanofoam structure (**3f**) is shown in Figure 9. The morphology of these nanofoams is quite interesting. Classical microphase separation models for block copolymers of this composition range predict a morphology ranging from spherical voids to an orthorhombic structure of short rods and eventually hexagonally packed cylinders, all depending on concentration.<sup>25</sup> The observed pores are irregularly shaped and show a small degree of interconnection, which slightly deviate from the predicted morphology. We suggest that the reason for this deviation from the expected spherical morphology is due to the formation of a nonequilibrium morphology. Microphase separation in nanofoams begins upon heating and solvent removal. Initially, there is sufficient chain mobility to allow phase separation

(24) Debye, P.; Bueche, A. M. *J. Appl. Phys.* **1940**, *20*, 518.

(25) Gallot, B. R. M. *Adv. Polym. Sci.* **1978**, *29*, 85.

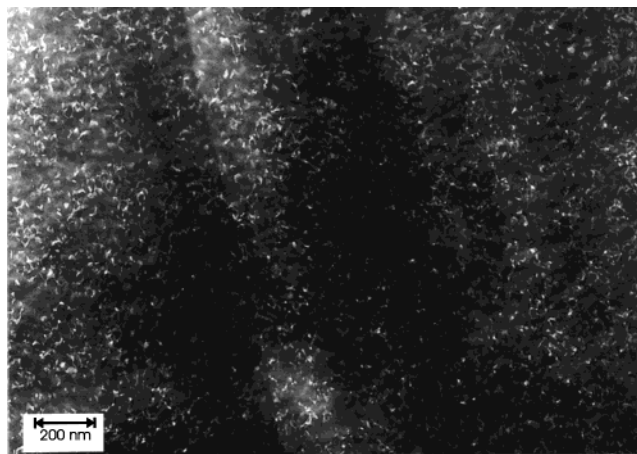


**Figure 9.** TEM micrograph of a 6FXDA/6FDAm polyimide nanofoam.

to begin. However, at a certain point, when the viscosity of the film becomes too high, molecular motion of the polymer chains decreases and the film is frozen into a nonequilibrium morphology.<sup>26</sup> The observed size and shape of the pores, 10–15 nm, matches very well with those determined by the SAXS experiments.

The lowered  $T_g$  of the nanofoams vs homopolymer led to concerns over the thermal stability of the final porous structure. In previous attempts to use highly ordered, anisotropic polyimides such as PMDA/ODA as nanofoam matrixes, porous structures were formed, but they were observed to collapse as the polymers were heated to temperatures well below the softening point of the polyimide matrix (softening point  $>450$  °C).<sup>27</sup> This collapse was found to be caused by stresses induced in the polymer film due to ordering of the polyimide at high temperatures. We believed that the amorphous, low-stress 6FXDA/6FDAm matrix would not be as likely to undergo stress-induced collapse. The 6FXDA/6FDAm nanofoam stability was studied as a function of density vs various annealing temperatures. Nanoporous polyimide samples were heated at intervals between 50 and 375 °C and held at each temperature for 2 h, and the density of the samples was remeasured. As shown in Figure 10, the nanofoam showed a modest degree of stability and it maintained 80% of its porosity when heated as high as its  $T_g$  (375 °C).

The dielectric constant of thin films of the nanofoams was studied as a function of temperature and frequency. The measurements were performed by spin-coating the copolymer onto glass slides with vacuum-deposited aluminum electrodes. The samples were thermally cured and then heated to effect pore generation. The second electrode was then evaporated, creating a capacitor configuration that was analyzed with a parallel plate dielectric resonator/oven assembly in conjunction with a HP4275A multifrequency LCR meter. With this apparatus, measurements of dielectric constant and dielectric loss as a function of temperature were possible.

Figure 11 shows the dielectric constant (at 1 MHz) of 6FXDA/6FDAm homopolymer and 6FXDA/6FDAm nano-

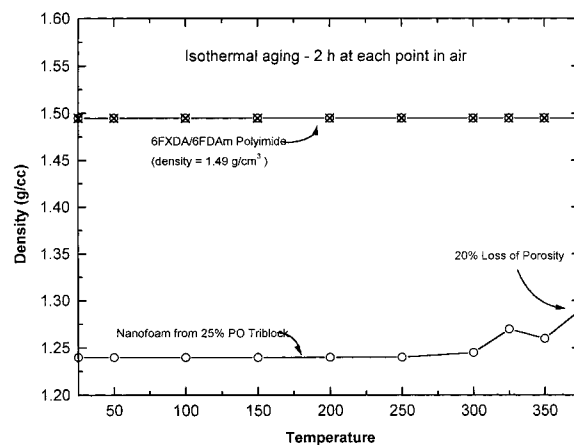


**Figure 10.** Thermal stability of a 6FXDA/6FDAm polyimide nanofoam.

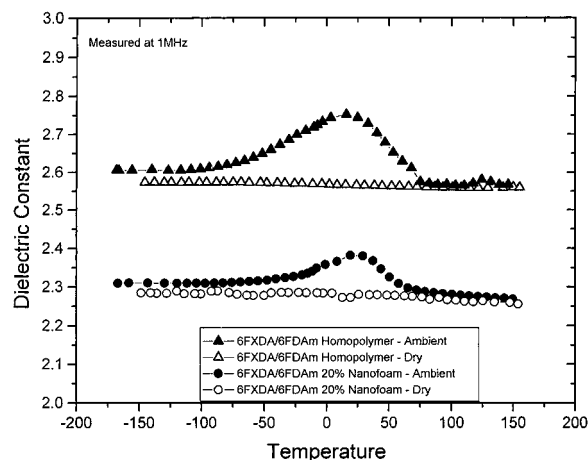


**Figure 11.** Dielectric constant of 6FXDA/6FDAm polyimide and a 6FXDA/6FDAm polyimide nanofoam as a function of temperature.

foam (4c) as a function of temperature. The room-temperature dielectric constant of the homopolymer is 2.75 after being stored in ambient conditions. As the sample is heated, the contribution to the dielectric constant arising from adsorbed moisture becomes apparent as water is released from the film, with the dielectric constant decreasing to a value of 2.56 at 150 °C. When kept moisture-free, the sample has a flat response in the range from  $-150$  to  $+150$  °C with a dielectric constant of 2.56. By comparison, the room-temperature dielectric constant of an ambient-stored 20% porous nanofoam is 2.39 prior to heating. Upon heating and loss of adsorbed water, the dielectric constant of the nanofoam drops to 2.27, with the dry sample showing a flat response in the range from  $-150$  to  $+150$  °C. The response of the samples was essentially the same for all measured frequencies (10 kHz–1 MHz). The contribution of water to the dielectric constant of the homopolymer ( $\Delta = 0.19$ ) was found to be greater than that found in the nanofoam sample ( $\Delta = 0.12$ ). This interesting observation indicates that atmospheric moisture is not preferentially aggregating in the nanofoam pores to any measurable extent. In fact, the data suggests that total water absorption is lower for nanofoams than for nonporous homopolymer. This behavior is not unique for this nanofoam system and the effect can be corroborated by quartz crystal microbalance (QCM). The water adsorption into thin nanoporous films

(26) Briber, R. M.; Fodor, J. S.; Russell, T. P.; Miller, R. D.; Hedrick, J. L. *Mater. Res. Soc. Symp. Proc.* **1997**, *461*, 272.

(27) Hedrick, J. L.; Russell, T. P.; Labadie, J. W.; Lucas, M.; Swanson, S. *Polymer* **1995**, *36*, 2685.



**Table 3. Refractive Index ( $\eta$ ) and Dielectric Constant ( $\epsilon$ ) Measurements**

sample	$\eta_{TE}$ (in-plane)	$\eta_{TM}$ (out-of-plane)	$\Delta\eta$	calcd $\epsilon$ (out-of-plane)	measd $\epsilon$ (out-of-plane)
6FXDA/6FDAm homopolymer ( <b>1</b> )	1.56	1.50	0.06	2.55	2.56
6FXDA/6FDAm nanofoam ( <b>4f</b> )	1.43	1.40	0.03	2.27	2.27

is currently being examined in a separate QCM study.<sup>28</sup> The porous sample shows a total reduction of the bulk dielectric constant ( $\Delta = 0.29$ ) for the sample containing 20% porosity.

To obtain a measure of the optical anisotropy of the thin films, their in-plane and out-of-plane refractive indices were measured with a commercially available Metricon prism coupler. In addition to obtaining an accurate measurement of the anisotropy (the difference between the in-plane and out-of-plane refractive indices), an estimate of the respective in-plane and out-of-plane dielectric constants can be obtained by applying the Maxwell equation,  $\epsilon \approx (\eta)^2$ , and correcting for frequency dispersions ( $\Delta\epsilon \cong +0.3$ ).<sup>29</sup> This type of analysis is very useful for rapid screening series of polyimide compositions, avoiding complex capacitance dielectric measurements. It is especially valuable for making comparative measurements on materials of similar chemical composition.

A comparison of the data calculated from refractive index measurements compared with actual measured dielectric constants is shown in Table 3. 6FXDA/6FDAm homopolymer has an in-plane refractive index,  $n_{TE}$ , of 1.56 and an out-of-plane refractive index,  $\eta_{TM}$ , of 1.50, showing that this polyimide is only slightly anisotropic ( $\Delta\eta = 0.06$ ). The expected drop in refractive index of samples upon pore formation was observed. A nanoporous sample of 6FXDA/6FDAm polyimide [derived from a 20% poly(propylene oxide) copolymer, sample 3] had

(28) Part of this study entitled Water Uptake in Thin Nanoporous Dielectrics by Quartz Crystal Microbalance, by K. R. Carter, M. Harbison, C. J. Hawker, J. L. Hedrick, R. D. Miller, and R. Waltman, was presented at the Materials Research Society National Meeting, San Francisco, CA, April 1999. Publication of these findings is forthcoming.

(29) Boese, D.; Lee, H.; Yoon, D. Y.; Swalen, J. D.; Rabolt, J. F. *J. Polym. Sci., Part B: Polym. Phys.* **1992**, *30*, 1321.

a measured in-plane refractive index,  $\eta_{TE}$ , of 1.43 and an out-of-plane refractive index,  $\eta_{TM}$ , of 1.40 ( $\Delta\eta = 0.03$ ). Thus, utilizing the modified Maxwell equation we were able to estimate this porous polyimide to have an out-of-plane dielectric constant of approximately 2.27 and that the homopolyimide would have a calculated dielectric constant of 2.55. For comparison, the reported measured out-of-plane dielectric constant,  $\epsilon$ , of the porous polyimide is 2.26 and that of the 6FXDA/6FDAm polyimide was 2.56, showing excellent agreement between the refractive index and dielectric constant measurements.

## Conclusions

The ability to prepare thin-film nanofoams of 6FXDA/6FDAm polyimide, with pores in the nanometer size range, has been demonstrated. 6FXDA/6FDAm/poly(propylene oxide) polyimide copolymers were made, cured to effect solvent removal with annealing at 310 °C under argon, and subsequently transformed into a porous structure by heating at 250 °C in air. The initial annealing at 310 °C allowed for solvent removal and the development of microphase separation in the polyimide matrix as evidenced by DMTA, SAXS, and TEM measurements. After pore generation, these nanofoam films could be subjected to further thermal treatments, even above the polyimide  $T_g$ , with only a small amount of pore collapse. With the incorporation of air pores, a lowering of the bulk dielectric constant of thin-film polyimide from 2.56 to 2.27 was accomplished, yielding new, low dielectric constant materials with pore stability in excess of 300 °C.

**Acknowledgment.** We thank Richard Siemens (IBM) for thermal gravimetric analyses, Hyuk-Jin Cha (LG Chemical Ltd.) for the tutorial on dielectric measurements, and Robert Briber at the University of Maryland for the TEM micrographs. Conversations with Thomas Russell (UMass, Amherst) were extremely valuable in discerning the SAXS data. We also acknowledge that this work was funded, in part, by NIST (ATP Contract 70NAAB-3H1-365).

CM990707O